Design of Photonic-Molecule-Based Multiway Beam Splitter/Coupler with Variable Division Ratio

Yury E. Geints *

Posted Date: 18 December 2023

doi: 10.20944/preprints202312.1274.v1

Keywords: photonics; beam splitter; beam coupler; photonic molecule; resonance; eigenmode; whisperring-galery mode

Article

Design of Photonic-Molecule-based Multiway Beam Splitter/Coupler with Variable Division Ratio

Yury E. Geints

V.E. Zuev Institute of Atmospheric Optics, 1 Acad. Zuev square, Tomsk, 634021, Russia

Abstract: Optical beam splitter is used for dividing an input optical beam into several separate beams with specific power ratio. Usually, conventional beam splitters have bulky dimensions and fixed dividing ratio which significantly limit the design of new miniaturized optical devices and integrated optical circuits. We propose and investigate a novel physical concept of a miniaturized planar optical splitter/coupler with a switching element in the form of a photonic molecule (PM) pair dispersing input optical fluxes along multiple ways with variable power proportions. The structural design of the proposed splitter is based on a silicon-on-insulator (SOI) platform and composed of high-quality resonators in the form of electromagnetically coupled submicron-sized microcylinders. The control on the power division ratio and the selection of optical beam directions is realized by tuning the photonic splitter structure to the corresponding resonance of PM supermode. Compared to known analogues, the proposed design is easy to fabricate, suitable for integration into a "System-on-a-chip" platform and can dynamically change the beam power division ratio by input wave-phase manipulation.

1. Introduction

Dielectric microresonators have long been actively used in disk lasers [1], high-resolution spectroscopy [2], laser frequency stabilization [3], add-drop filters for compact wavelength division (de)multiplexing [4, 5], dispersion compensation of optical fiber transmission lines [6], implementation of all-optical switching for optical signals [7, 8], optical nodes of quantum computers [9], as well as beam power dividers [10, 11] and inertia-free optical couplers [12, 13].

Generally, an optical beam splitter (BS) is a device for splitting an optical beam incident on its input port into two or more separate beam(s) with specific power ratio(s) and optionally field polarization states. Typically, glass plates or prisms with semi-reflective coatings are used in the design of beam splitters. However, in the spatial scales of nanophotonics devices, as well as in the geometry of planar on-chip optical elements, the bulky dimensions of conventional beam splitters and their usually fixed power division ratio significantly limit the design of new miniaturized optical devices and make it difficult to build integrated optical circuits. This challenge has stimulated the development of BS-devices based not on differential refraction of optical fluxes but on the principle of diffraction division of an input optical signal into separate beamlets by interaction (transmission) with specially designed diffractive optical elements (DOEs). Thus, such DOEs can be, e.g., ring resonators integrated into photonic crystals [14, 15], specially shaped reflecting/transmitting metasurfaces and meta-lattices [11, 16, 17] providing angular beam separation, as well as planar conventional Y-branch splitters with a complex hierarchy [18].

Recently, optical splitters based on planar disk or ring traveling/standing wave resonators realized as an integrated element inside photonic crystals [8, 15] or directly on a silicon-on-insulator (SOI) platform [4, 5, 19] have become widespread. Typically, such splitters function in a narrow spectral range near the eigenmode resonances of a microcavity, when the incoming optical radiation is coupled to the resonant modes and redirected into signal collection channels (drop ports). The main advantages of such BS devices are their planar design suitable for operation directly as part of a photonic SOI microchip, as well as low insertion losses of the optical signal, typically < -8 dB. Another profit of resonance-based dividers is that they can function as narrow passband filters allowing an optical signal passing only within the resonance contour of cavity eigenmode.

The most common structural design of resonant beam splitters (RBS) is usually composed of several high-quality (high-*Q*) resonant DOEs (ring, disk, microcylinder, microsphere) coupled to the commutation buses in the form of rectangular or cylindrical waveguides forming the through and drop-ports of the optical signal output. The resonators themselves are usually in close subwavelength contact with each other in a serial [4] or parallel structural topology [5, 20]. In optical splitters based on multimode interaction, the interconnection of resonant elements and waveguide buses is realized by indirect coupling of evanescent electromagnetic fields of the eigenmodes. The presence of several resonators in the RBS design improves its filtering properties. At the same time, the topologies of dividers and couplers with nested [21] and cascade-arranged microrings [22] are also reported, which possess increased sensitivity of the whole device.

At the same time, specific photonic structures - photonic molecules (PM), formed by electromagnetic coupling of two or more optical microcavities have recently gained increasing scientific interest [23, 24]. This physical molecular analogy stems from the special optical PM properties which are manifested themselves in the fact that the normal electromagnetic modes of a PM constituted of several interacting "photonic atoms" and the electronic states of real atoms of matter combined into a molecule behave in a similar way. In other words, a single optical resonator is treated as a photonic atom, while several optically coupled resonators are treated as the photonic analog of a matter molecule. With these high-dimensionality of composite structures, controlled interactions between light and matter can be achieved and even enhanced by manipulating the coupling or matching of individual resonators including their mechanical and optical tuning [25-27].

To date, quite a few different topological forms of PMs are studied including basic diatomic molecules, molecular chains, and complex 2D structures [28]. Meanwhile, a common property of all PMs is the appearance of specific structural electromagnetic superlattice modes, usually referred to as the supermodes, resulting from the collective resonant interaction of the optical fields of all atoms in a photonic molecule [29]. This strong coupling produces a new hybridized spectrum of eigenfrequencies of molecular photonic structure as a whole [26]. PM supermodes differ in the type of optical coupling of atoms and form bonding (even) and anti-bonding (odd) modes, which means the corresponding symmetry or antisymmetry of the electric field distribution with respect to PM axis [30]. In addition, with the change of the type of interatomic coupling, the quality factor (*Q*) of PM supermodes also changes demonstrating in some cases a drastic increase relative to the *Q*-value of an isolated resonator [25, 31].

Typically, photonic molecules are excited using a single optical channel through a PM matched tapered fiber [26], or by illuminating the molecule with free-space coupled radiation [32]. Recently, in our work [31] a scheme using simultaneously two optical buses with varying phase difference was proposed to enhance or suppress the generation of certain supermodes of the molecule and thus control its spectral response. According to the structural parameters, the photonic molecules consisting of planar resonators are similar to the resonant beam splitters discussed here. Both photonic structures have coupling resonant cavities and excitation/emission channels. In this connection, however, the possibility of using PMs with complex topology possessing rich spectrum of supermodes as an element of RBS has not yet been discussed in the literature.

In this paper, we propose a new theoretical concept of a resonant optical beam power splitter based on the photonic molecules (PM-BS) with different topologies. We consider a PM formed by quazi-planar resonators in the form of several silicon microcylinders with subwavelength thickness. The main advantage of the proposed PM-based optical splitter over known analogs is its multiway operation, which allows redirecting the input optical signal into several oppositely directed drop channels with varying power ratio. Additionally, by adding another input channel, PM-based beam splitter can function as an optical coupler, which mixes signals from the input ports and directs them to one or more output channels. Unlike similar metasurface-based beam dividers [33, 34] in terms of the functionality, the proposed beam splitter is much simpler and cheaper in fabrication, suitable for the “System-on-a-chip” integration, and can dynamically change its power splitting ratio by spectrally tuning to a different resonant supermode of the constituting PM. Moreover, another advantage of the proposed RBS is its ultra-compact design with the dimensions typically not

Preprints (www.preprints.org) | NOT PEER-REVIEWED | Posted: 18 December 2023 doi:10.20944/preprints202312.1274.v1

exceeding several optical wavelengths as compared to the optical splitter based on ring resonators [5].

2. PM-BS structural model and working principle

Without reducing the generality of the problem considered, we further analyze a certain PM topology built from identical photonic atoms in the form of a circular cylinder of a diameter, say, $D = 1200$ nm and height $h = 600$ nm placed in the nodes of a rectangular 2D-lattice with the period $d = 1270$ nm. Different number of PM atoms can form photonic structures with either two or four interacting resonators. According to the physical type of this optical field coupling, we will refer to the serial arrangement of atoms as "2*s*" and "4*s*" configurations as depicted in Fig. 1(a) and (b), whereas a mixed type of serial-parallel bonding is labeled as "2*s*-*p*" molecule and shown in Fig. 1(c).

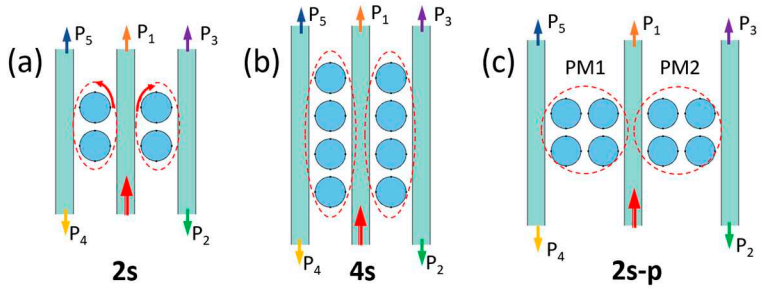

Figure 1. Structural types of PM-based optical splitters with (a, b) serial (2*s* and 4*s*), and (c) serial-parallel (2*s*-*p*) electromagnetic coupling of atoms in photonic molecules PM1 and PM2 (outlined with dashed ovals). Optical signal is injected through the central waveguide (red arrow) and collected in the through and drop ports labeled as P_1 and P_2 to P_5, respectively.

PM is assembled on the SOI platform with a silicon dioxide (SiO_2) substrate and is structurally characterized by the interatomic gap, $g = 300$ nm. Crystalline silicon (Si) with refractive index $n = 3.5$ and almost zero optical absorption ($\kappa \sim 10^{-11}$) in the telecommunication spectral band centered on the wavelength $\lambda = 1330$ nm [35] is chosen as the material for photonic atoms. To enhance the functionality, the considered photonic splitter is composed of two PMs coupled through a central waveguide (Fig. 2a,c) acting as an input port. On the lateral sides of the splitter structure, two more waveguides are mounted at certain distance from the outermost atoms (250 nm) serving for the collection the divided optical beams. All waveguides can be fabricated from the core of a single-mode optical fiber (SiO_2), or through the etching of a dielectric photoresist (e.g., PMMA). The refractive index of the waveguides during the simulation is chosen as $n_1 = 1.5$.

Preprints (www.preprints.org) | NOT PEER-REVIEWED | Posted: 18 December 2023 doi:10.20944/preprints202312.1274.v1

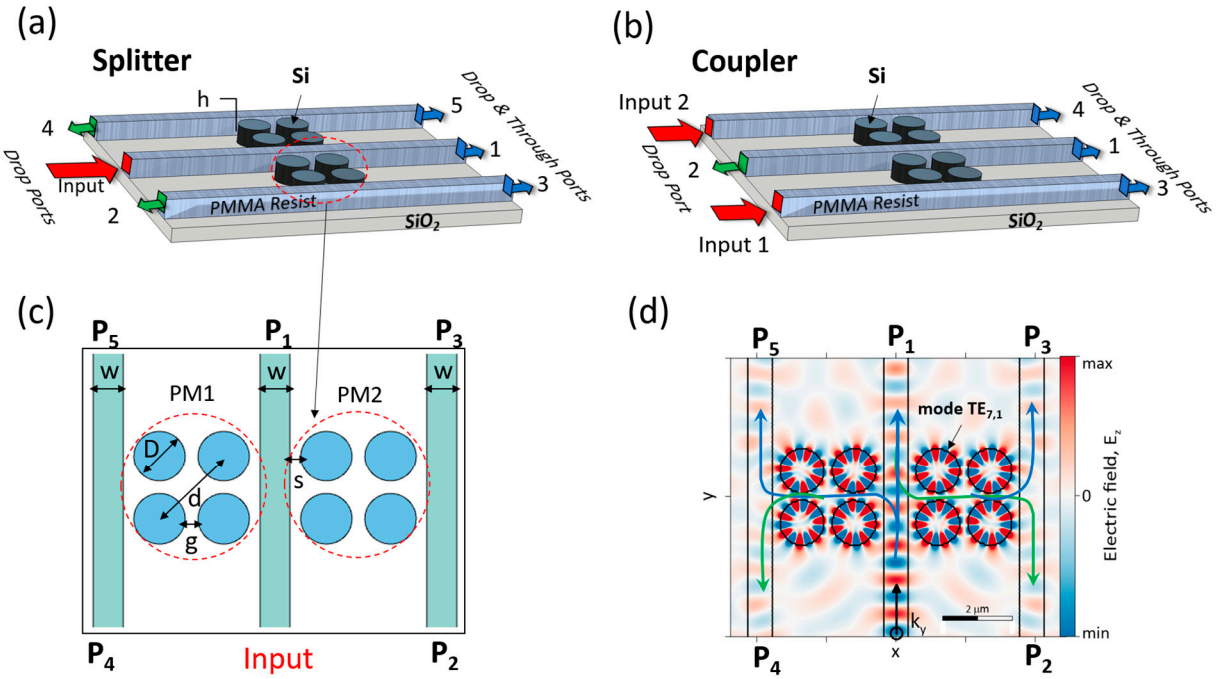

Figure 2. 3D-design of proposed photonic (a) splitter and (b) coupler on the SOI platform with input and drop ports labeling. (c) PM-BS structural scheme and (d) the working principle.

An optical wave with TE-mode polarization (Fig. 2d) having an electric field vector directed along *z*-axis (out of the plane of the figure) is fed to the input of the splitter. After interacting with the resonant structure (PM), the divided optical fluxes are captured by the through and drop ports 1 to 5. When operating as a coupler (Fig. 2b), the operation order of optical ports is reversed. Now, ports 4 and 2 become input ports and the remaining ports become signal acquisition ports.

The spectral range of the input wave is chosen to include one of the high-*Q* eigenmode resonances of the cylindrical atom. This resonant mode exists in the form of a standing or traveling wave and is often referred to as the "whispering-gallery mode" (WGM) [36]. In order for the PM to function as a coherent resonant photonic structure, it is necessary to require a sufficiently high-*Q* values of the microcavity used to ensure the WGM excitation. Since the surface of a dielectric atom is not totally reflective, the optical fields of the eigenmodes leak out the resonator boundaries and in this sense the WGMs in an open resonator are the quasi-bounded or quasi-normal electromagnetic modes. The optical coupling between the PM atoms is precisely due to these leaking evanescent fields [37]. Thus, in the situation considered the eigenmode $TE_{7,1}$ in a silicon cylinder is chosen as the fundamental resonance (Fig. 2d) having quality factor $Q = 8500$ at the wavelength $\lambda = 1338.2$ nm. Note, that according to the adopted notations for the electromagnetic eigenmodes of a sphere, the subscripts "7,1" denote the semi-number of optical standing wave antinodes along the azimuthal direction (along the cylinder rim) and the number of maxima along the radial coordinate, respectively.

The numerical solution of the Helmholtz wave equation for the electromagnetic field in the investigated photonic structure is performed using the Wave Optics module of COMSOL Multiphysics 5.1 software, which exploits the finite element method (FEM). Without limiting the generality, we use the 2D formulation of the problem as shown in Figs. 2(c, d). In this case, the whole photonic structure is surrounded by a rectangular region of perfectly absorbing layers (PML) to prevent wave reflection from the boundaries. The optical radiation is input through the corresponding COMSOL digital ports. For the numerical discretization of all simulation domains a mesh with triangular elements and a maximum edge size of $\lambda/40$ is used. The wavelength sweep is performed by creating a parametric study in the range of $1333 \text{ nm} \le \lambda \le 1343 \text{ nm}$, which includes all supermodes of the considered PM topologies based on the $TE_{7,1}$ resonance of single atom.

Preprints (www.preprints.org) | NOT PEER-REVIEWED | Posted: 18 December 2023 doi:10.20944/preprints202312.1274.v1

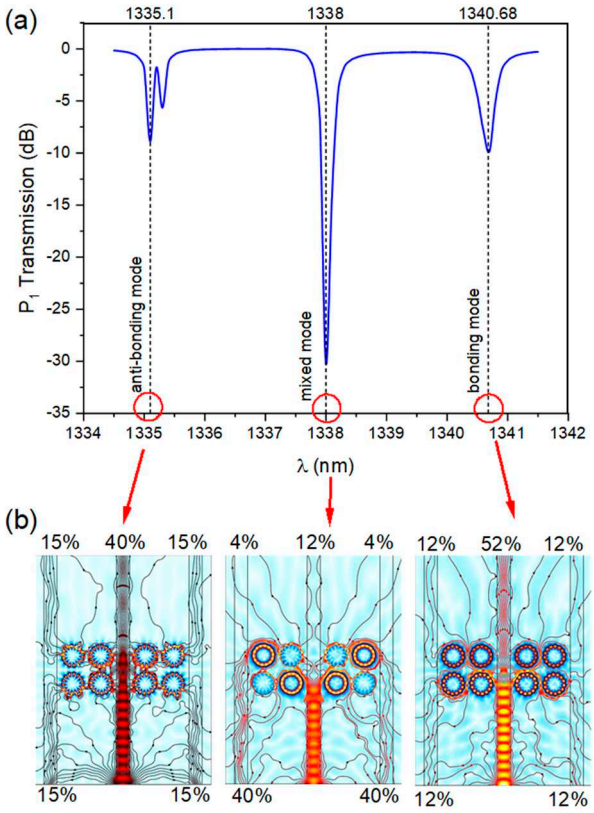

Figure 3. (a) Resonance spectrum of a 2*s*-*p* photonic molecule showing different types of supermodes. (b) 2D-distributions of the normalized amplitude $|E_z|$ (color maps) and the Poynting vector $\mathbf{S}(x,y)$ for three principal PM supermodes. The numbers indicate the proportions of the optical energy splitting which is inputted through central waveguide.

To understand the PM-BS operation principle, we consider the resonance spectrum of a 2*s*-*p* molecule, which is shown in Fig. 3(a) as the dependence of P_1-port transmittance on the optical wavelength. As seen, the spectrum of such a molecule contains a total of 4 collective supermodes, each of them being fourfold degenerate due to high spatial symmetry of the PM atomic structure. Here, three groups of resonant supermodes can be distinguished [31]: (i) anti-bonded modes with $\lambda = 1335.1$ nm and 1335.3 nm, (ii) bonded modes with $\lambda = 1340.68$ nm, and (iii) a mixed type supermodes centered at $\lambda = 1338$ nm.

In the anti-bonded molecular supermode the phases of field oscillations in all atoms are opposite and mirror-symmetric with respect to the symmetry axis of the molecule. Practically, the anti-bonded supermode can be considered as the eigenmode resonance of the half-PM located near a perfectly reflecting mirror. Previously [38] on the example of a dielectric sphere on a mirror it was shown, that in this case the blue shift of TE-mode resonance is realized. Similar effect is observed for the anti-bonded supermode of a photonic molecule. In contrast, the bonded supermode is red-shifted within the PM spectrum and demonstrates the appearance of strong bonds between electric fields of atoms. As in an ordinary molecule of a matter, a PM exhibits strong interference and hybridization of optical eigenmodes (molecular energy terms), which is expressed in mode splitting and appearance of new collective field oscillations (low-energy sublevels). The mixed-type PM supermode bears the imprint of both bounded and anti-bounded modes, and the distribution of interatomic optical fields here is characterized simultaneously by symmetry along one direction and antisymmetry with respect to another plane.

In Fig. 3(b), the streamlines of the Poynting vector are plotted for each of the selected supermodes, defined as $\mathbf{S} = (c/8\pi)\,\mathrm{Re}\left[\mathbf{E}\times\mathbf{H}^{*}\right]$, where $\mathbf{E}$ and $\mathbf{H}$ are electric and magnetic field vectors, respectively, and c is the speed of light. It can be seen that in resonance, the streamlines of vector $\mathbf{S}$ are captured from the feed waveguide by nearby atoms of the molecule and then directed

Preprints (www.preprints.org) | NOT PEER-REVIEWED | Posted: 18 December 2023 doi:10.20944/preprints202312.1274.v1

into the hybridized field of PM supermode formed by the coupling of atomic resonant modes. Photonic molecules on both sides of the feed waveguide always have a counter-directed circulation of optical energy and produce the regions of field singularity such as optical vortices and saddles, which is typical for standing-wave resonators [38]. The most distant atoms of photonic molecules (relative to input waveguide) drop a part of the energy flux into the lateral waveguides and the rest of mode optical energy is looped again in the molecular supermode.

It is also clearly visible that the PM-BS structure disperses the optical fluxes to all ports in both forward and reverse directions in different proportions, which depend on the particular excitation supermode. Consequently, the splitting ratio of the input optical signal can be controlled by varying the optical wavelength. This is one of the main advantages of the proposed photonic structure.

3. Structural types of PM-based beam splitter

Worthwhile noting, the presence even in the simplest diatomic molecule of two coupled resonant microcavities not only enriches the spectrum of its electromagnetic modes but also opens new paths of the optical energy transportation. This is illustrated in Figs. 4(a,b), which show the most important characteristic of the optical splitter, the split ratio, for two photonic structures assembled from (i) a pair of ring resonators similar to that proposed in Refs. [5, 22], and (ii) two PMs of 2*s* type. Different color bars indicate the relative fraction of the total optical power directed to the corresponding splitter port. The negative values correspond to reverse power directed into ports 2 and 4.

Clearly, for a two-ring splitter one can obtain only single dividing proportion between the optical ports, namely (rounded) 1:3:0:3:0, as shown in the schematic of Fig. 4(a). In other words, at the resonance of this structure (λ = 1338.3 nm) nearly 6/7 of total input beam power is reversed into the drop ports 2 and 4, while 1/7 of total power passes through into port 1. The beam power practically does not enter the through ports 3 and 5, i.e. such a photonic structure works as a resonant filter [5].

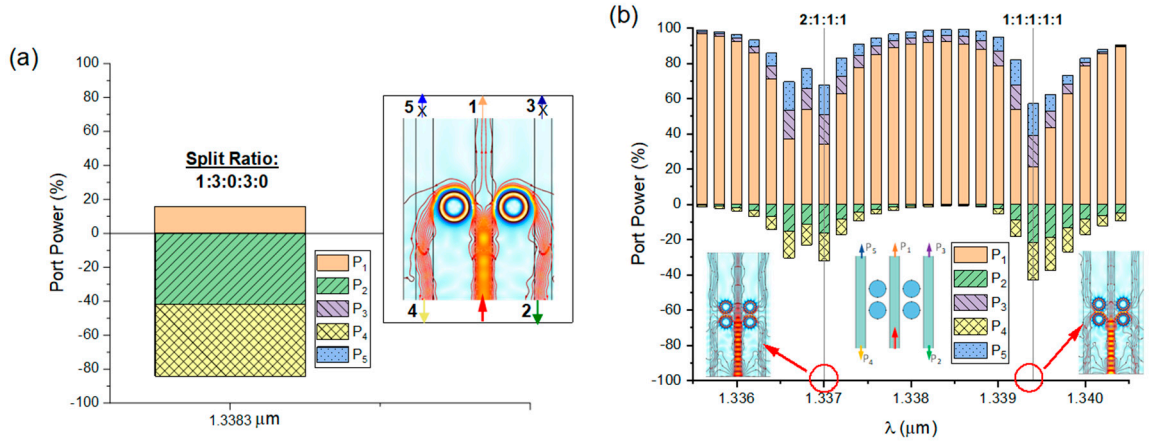

Figure 4. (a) Splitting ratio for a pair of microrings in resonance. The inset shows the Poynting vector streamlines. (b) Spectral dependence of the relative power directed in the ports of proposed PM-BS based on two diatomic 2*s*-PM. **S** streamlines are shown for the two supermode resonances.

A completely different situation is observed in the PM-based splitter shown in Fig. 4(b). Here, two high-quality ($Q \sim 10^5$) resonances at the wavelengths 1337 nm and 1339.4 nm can be found in BS spectral response function. At each of these supermodes, a different beam splitting is realized. Importantly, at the red-shifted bonded supermode the input beam is divided equally among all ports of the splitter, while at the blue-shifted anti-bonded resonance the power in the pass-through port is twice as high as that in remaining drop ports. Meanwhile, out of resonance the majority of input power passes unchanged into port 1, and the photonic splitter is in the *off-line* state.

The analysis of Poynting streamline maps shows that in the case of the anti-bonded resonance, the input optical energy flux is equally divided between the upper and lower parts of the photonic

Preprints (www.preprints.org) | NOT PEER-REVIEWED | Posted: 18 December 2023 doi:10.20944/preprints202312.1274.v1

molecule because the optical fields of molecule parts are in antiphase. In contrast, at the resonance of the lower-frequency bonded supermode, the fields of atoms and both (left/right) molecules are phase-matched and constructively interfere in the region of the input central waveguide which leads to the division ratio change towards higher power in the through port 1.

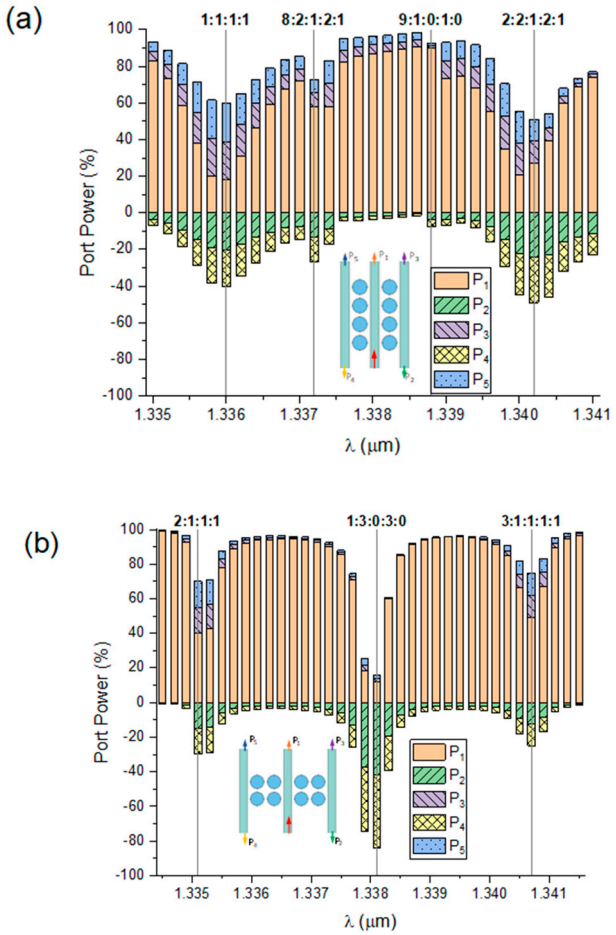

Figure 5. Spectral dependence of the dividing ratio of PM-PS designed on a pair of (a) 4*s* and (b) 2*s*-*p* molecules.

In Figs. 5(a,b), the working diagrams of splitters based on photonic molecules of 4*s* and 2*s*-*p* types are plotted. The splitting coefficients realized for the main resonances of these photonic structures are highlighted. Obviously, different molecular structures and different supermodes of the molecules produce very different splitting ratios of the input beam power into the output waveguides. Indeed, it is possible to obtain an equal power distribution among all ports (ratio 1:1:1:1:1 at $\lambda = 1336$ nm of 4*s*-molecule), shifting the dividing balance toward the pass-through port (ratio 2:1:1:1:1 at $\lambda = 1335.1$ nm and 3:1:1:1:1 at $\lambda = 1340.7$ nm of molecule 2*s*-*p*), or redirecting the divided optical beams predominantly toward retro-ports 2 and 4 (ratio 1:3:0:3:0 for 1338.1 nm mode of molecule 2*s*-*p*, and ratio 2:2:1:2:1 at $\lambda = 1340.2$ nm in molecule 4*s*).

Moreover, the spectral position and quality factor of the supermodes in PM with selected topology can be easily tuned by the interatomic gap (g) adjustment [Geints2023tyr]. Importantly, we have performed the stability analysis of PM structure to the fabrication errors related with random deviations of atomic position, which is controlled by the g-parameter. It turns out, that the tolerance of the supermode resonance to random shifts in the interatomic gap is about 10 nm for the anti-bonded and bonded modes, whereas only 70 nm changes in g could spoil central mixed supermode. Such structural tolerances are quite achievable in modern ion/electron beam lithography processes.

4. Design of PM-based optical coupler

Preprints (www.preprints.org) | NOT PEER-REVIEWED | Posted: 18 December 2023 doi:10.20944/preprints202312.1274.v1

Now recall the switching photonic structure shown in Fig. 2(b). Such a device allows all-optical mixing and switching of different optical signals through the interference coupling into single molecular supermode. In this case, two optical beams are input to the coupler, and demultiplexing is performed in ports 1 through 4. Note, here we do not consider the design of a classical multi-frequency add-drop filter, but assume that both input optical signals are at the same wavelength. The relative power arriving at the optical ports of the coupler based on th photonic molecule pair having two and four atoms (2*s* and 4*s* molecules) is shown in Figs. 6(a,b) as a function of the input radiation wavelength.

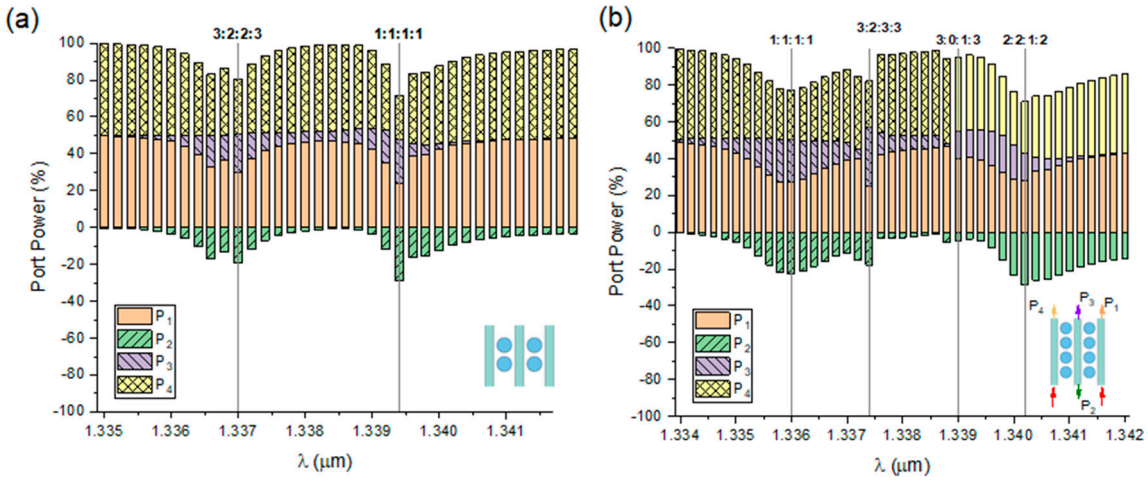

Figure 6. Spectral dependence of relative optical power in the output ports of PM-based coupler for (a) 2*s* и (b) 4*s* PM structures.

Evidently, the distribution of optical fluxes during their coupling occurs in a similar way as in the optical splitter discussed above, except that the coupler always operates symmetrically, i.e. the power in pass-through ports 1 and 4 is always the same. Only the mutual proportion of optical beams directed to the drop channels 2 and 3 changes.

Preprints (www.preprints.org) | NOT PEER-REVIEWED | Posted: 18 December 2023 doi:10.20944/preprints202312.1274.v1

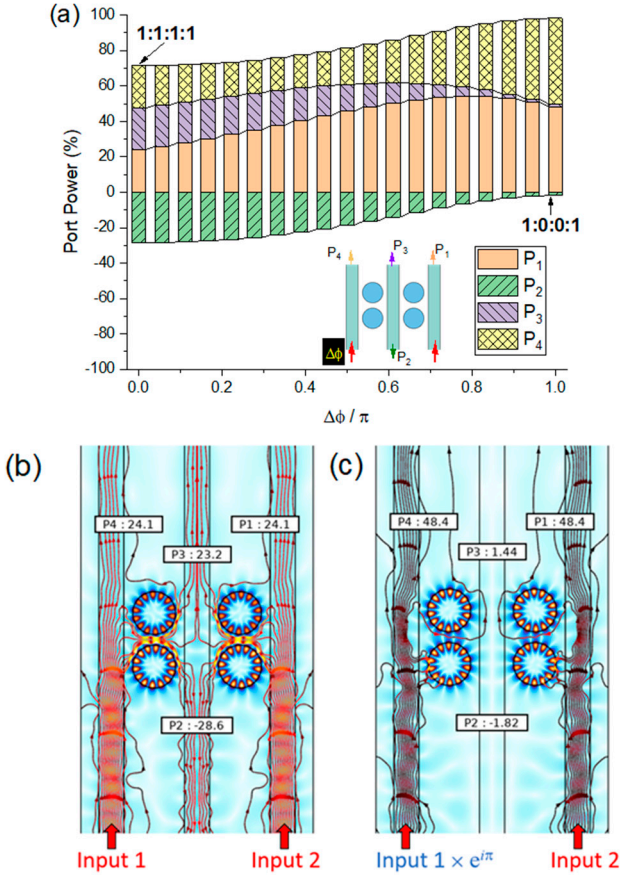

Figure 7. (a) Dependence of relative power in the optical ports of optical coupler on the left port dephasing Δϕ. (b-c) Poynting vector streamlines in the 2*s*-PM coupler at (b) Δϕ = 0 and (c) Δϕ = π radians at 1339.4 nm bonded supermode resonance.

Interestingly, if a phase shift is introduced in one of input optical ports, as shown in Fig. 7(a), the PM optical coupler becomes the ability for adjusting the fraction of power directed into each output port separately. Indeed, when the phase of the input ports is matched (Δϕ = 0, Fig. 7b), the incoming optical flux is equally divided between the upper and lower PM atoms, and then constructively interfere within central waveguide to form equal-power beams in opposite directions. Controversially, when the input ports are operating in antiphase (Δϕ = π, Fig. 7c), the supermode optical fields of left and right molecules cancel each other out in the coupling area, and thus power output to ports 2 and 3 nearly terminates and the signals at these ports drop to ~ -17 dB. In intermediate situations, Δϕ < π, a smooth adjustment of the power proportion in each of the output ports can be realized. Importantly, when the photonic coupler is tuned to a different resonance, particularly the anti-bonded supermode (1337 nm), the considered structure functions in a mirror image manner with the same variation in phase delay between 0 and π radians.

5. Conclusion

In summary, we present the physical concept of a micrometer-scale planar optical splitter/coupler-on-photonic molecule that distributes one or two input optical beams to multiple routes with variable power ratios. A structural design of such a photonic device on SOI platform is proposed. The power division ratio of input beams is controlled by tuning the structure to the corresponding resonance of the photonic molecule hybridized supermode. Compared to known analogs, the proposed conceptual model is characterized by relative simplicity and cheapness in

fabrication, is suitable for integration into a "system-on-a-chip" platform, can dynamically change the beam power division ratio, and is able to produce counter-directional optical flows.

Funding. Ministry of Science and Higher Education of the Russian Federation (IAO SB RAS).

Disclosures. The author declares no conflicts of interest.

Data availability. Data underlying the results presented in this paper may be obtained from the authors upon reasonable request.

References

1. A. Pasquazi, M. Peccianti, L. Razzari, D.J. Moss, S. Coen, M. Erkintalo, Y.K. Chembo, T. Hansson, S. Wabnitz, P. Del'Haye, X. Xue, A.M. Weiner, R. Morandotti, "Micro-combs: A novel generation of optical sources," Phys. Rep. 729 1–81 (2018), http://dx.doi.org/10.1016/j.physrep.2017.08.004.
2. Z. Xia, A.A. Eftekhar, M. Soltani, B. Momeni, Q. Li, M. Chamanzar, S. Yegnanarayanan, and A. Adibi, "High resolution on-chip spectroscopy based on miniaturized microdonut resonators," Opt. Express 19, 12356-12364 (2011), https://doi.org/10.1364/OE.19.012356
3. V. V. Vasiliev, V. L. Velichansky, V. S. Ilchenko, M. L. Gorodetsky, L. Hollberg, and A. V. Yarovitsky, "Narrow-line-width diode laser with a high-Q microsphere resonator," Opt. Commun. 158, 305–312 (1998)
4. M. A. Popovic, T. Barwicz, M.S. Dahlem, F. Gan, C.W. Holzwarth, P.T. Rakich, H.I. Smith, E.P. Ippen and F.X. Kartner, "Tunable, fourth-order silicon microring-resonator add-drop filters," 33rd European Conference and Exhibition of Optical Communication, Berlin, Germany, 2007, pp. 1-2, doi: 10.1049/ic:20070077.
5. A. Bagheri, F. Nazari and M.K. Moravvej-Farshi, "Bidirectional switchable beam splitter/filter based graphene loaded Si ring resonators," Phys. Scr. 96 125536 (2021), https://doi.org/10.1088/1402-4896/ac42a8
6. C. K. Madsen and G. Lenz, "Optical all-pass filters for phase response design with applications for dispersion compensation," IEEE Photon. Technol. Lett. 10, 994–996 (1998), https://doi.org/10.1109/68.681295
7. J.E. Heebner and R.W. Boyd, "Enhanced all-optical switching by use of a nonlinear fiber ring resonator," Opt. Lett. 24, 847-849 (1999), https://doi.org/10.1364/OL.24.000847
8. M.K. Chhipa, B.T.P. Madhav, B. Suthar, "An all-optical ultracompact microring-resonator-based optical switch," J. Comput. Electron. 20, 419–425 (2021). https://doi.org/10.1007/s10825-020-01628-w
9. D. Grassani, S. Azzini, M. Liscidini, M. Galli, M.J. Strain, M. Sorel, J.E. Sipe, and D. Bajoni, "Micrometer-scale integrated silicon source of time-energy entangled photons," Optica 2, 88-94 (2015), https://doi.org/10.1364/OPTICA.2.000088
10. V.S.P. Kumar, P. Sunita, M. Kumar, N. Kumari, V. Karar, A.L. Sharma, "Design and fabrication of multilayer dichroic beam splitter," Adv. Mater. Proc. 2, 398 (2017), https://doi.org/10.5185/amp.2017/610
11. X. Chen, H. Zou, M. Su, L. Tang, C. Wang, S. Chen, C. Su, Y. Li, "All-Dielectric Metasurface-Based Beam Splitter with Arbitrary Splitting Ratio," Nanomaterials 11, 1137 (2021). https://doi.org/10.3390/nano11051137
12. Y. Wang, L. Xu, H. Yun, M. Ma, A. Kumar, E. El-Fiky, R. Li, N. Abadíacalvo, L. Chrostowski, N. A. F. Jaeger, and D. V. Plant, "Polarization-independent mode-evolution-based coupler for the silicon-on-insulator platform," IEEE Photon. J. 10, 4900410 (2018), https://doi.org/10.1109/JPHOT.2018.2835767
13. C. Pérez-Armenta, A. Ortega-Moñux, J.M. Luque-González, R. Halir, P.J. Reyes-Iglesias, J. Schmid, P. Cheben, Í. Molina-Fernández, and J.G. Wangüemert-Pérez, "Polarization-independent multimode interference coupler with anisotropy-engineered bricked metamaterial," Photon. Res. 10, A57-A65 (2022), https://doi.org/10.1364/PRJ.446932
14. T.A. Moniem, "All-optical digital 4 × 2 encoder based on 2D photonic crystal ring resonators," J. Mod. Opt. 63(8), 735–741 (2016), https://doi.org/10.1080/09500340.2015.1094580
15. B. Rahmi, H. Badaoui, M. Abri, A. Imam, "High-performance all-optical 3×8 photonic crystal decoder using nonlinear micro-ring resonators," App. Phys. B 129:35 (2023), https://doi.org/10.1007/s00340-023-07981-5
16. W. Xu, L. Hu, K. Shao, H. Liang, T. He, S. Dong, J. Zhu, Z. Wei, Z. Wang, and X. Cheng, "Design of arbitrary energy distribution beam splitters base on multilayer metagratings by a hybrid evolutionary particle swarm optimization," Opt. Express 31, 41339-41350 (2023), https://doi.org/10.1364/OE.502125
17. Y. Ren, Z. Liang, X. Shi, F. Yang, X. Zhang, R. Dai, S. Zhang and W. Liu, "Infrared All-Dielectric Metasurface Beam Splitter Based on Transflective Structures. Appl. Sci. 13, 5207 (2023). https://doi.org/10.3390/app13085207
18. Y. Xu, Z. Tian, X. Meng and Z. Chai, "Methods and applications of on-chip beam splitting: A review," Front. Phys. 10:985208 (2022). https://doi.org/10.3389/fphy.2022.985208

19. B. E. Little, S. T. Chu, P. P. Absil, J. V. Hryniewicz, F. G. Johnson, F. Seiferth, D. Gill, V. Van, O. King, and M. Trakalo, "Very high-order microring resonator filters for WDM applications," in IEEE Photonics Technology Letters, vol. 16, no. 10, pp. 2263-2265 (2004), http://doi.org/10.1109/LPT.2004.834525
20. Z. Peng, T. Arakawa, "Tunable Vernier Series-Coupled Microring Resonator Filters Based on InGaAs/InAlAs Multiple Quantum-Well Waveguide," Photonics 10(11):1256 (2023), https://doi.org/10.3390/photonics10111256
21. M.A. Selim and M. Anwar, "Enhanced Q-factor and effective length silicon photonics filter utilizing nested ring resonators," J. Opt. 25, 115801 (2023), https://doi.org/10.1088/2040-8986/acf5fd
22. L. Jin, M. Li, J.-J. He, "Highly-sensitive silicon-on-insulator sensor based on two cascaded micro-ring resonators with vernier effect," Opt. Commun. 284, 156-159 (2011), https://doi.org/10.1016/j.optcom.2010.08.035
23. Y. P. Rakovich and J. F. Donegan, "Photonic atoms and molecules," Laser Photon. Rev. 4, 179–191 (2010).
24. K. Liao, X. Hu, T. Gan, Q. Liu, Z. Wu, C. Fan, X. Feng, C. Lu, Y. Liu, and Q. Gong, "Photonic molecule quantum optics," Adv. Opt. Photon. 12, 60-134 (2020).
25. S.V. Boriskina "Theoretical prediction of a dramatic Q-factor enhancement and degeneracy removal of whispering gallery modes in symmetrical photonic molecules," Opt. Lett. 31, 338 (2006);
26. Y. Li, F. Abolmaali, K. W. Allen, N.I. Limberopoulos, A. Urbas, Y. Rakovich, A.V. Maslov, V.N. Astratov, "Whispering gallery mode hybridization in photonic molecules," Laser Photonics Rev. 11, 1600278 (2017). https://doi.org/10.1002/lpor.201600278
27. Y.E. Geints, "Manipulating the supermodes in photonic molecules: prospects for all-optical switching and sensing," J. Opt. Soc. Am. B 40, 1875-1881 (2023), https://doi.org/10.1364/JOSAB.491320
28. Photonic Microresonator Research and Applications (Eds. I. Chremmos, O. Schwelb, N. Uzunoglu) // Springer Series in Optical Sciences (Springer, LLC 2010).
29. P. W. Evans and N. Holonyak, "Room temperature photopumped laser operation of native-oxide-defined coupled GaAs-AlAs superlattice microrings," Appl. Phys. Lett. 69, 2391–2393 (1996).
30. M. Bayer, T. Gutbrod, J. P. Reithmaier, A. Forchel, T. L. Reinecke, P. A. Knipp, A. A. Dremin, and V. D. Kulakovskii, "Optical modes in photonic molecules," Phys. Rev. Lett. 81, 2582–2585 (1998).
31. Y.E. Geints, "Phase-controlled supermodes in symmetric photonic molecules," JQSRT 302, 108524 (2023), https://doi.org/10.1016/j.jqsrt.2023.108524
32. T. X. Hoang, H.-S. Chu, F. J. García-Vidal and C. E. Png, "High-performance dielectric nano-cavities for near- and mid-infrared frequency applications," Opt. 24 094006 (2022).
33. X. Chen, H. Zou, M. Su, L. Tang, C. Wang, S. Chen, C. Su, Y. Li, "All-Dielectric Metasurface-Based Beam Splitter with Arbitrary Splitting Ratio," Nanomaterials 11, 1137 (2021), https://doi.org/10.3390/nano11051137
34. T. Tian, Y. Liao, X. Feng, K. Cui, F. Liu, W. Zhang, Y. Huang, "Metasurface-Based Free-Space Multi-Port Beam Splitter with Arbitrary Power Ratio," Adv. Optical Mater. 11, 2300664 (2023), https://doi.org/10.1002/adom.202300664
35. C. Schinke, P. C. Peest, J. Schmidt, R. Brendel, K. Bothe, M. R. Vogt, I. Kröger, S. Winter, A. Schirmacher, S. Lim, H. T. Nguyen, D. MacDonald. "Uncertainty analysis for the coefficient of band-to-band absorption of crystalline silicon," AIP Advances 5, 67168 (2015): https://doi.org/10.1063/1.4923379
36. A. B. Matsko and V. S. Ilchenko, "Optical resonators with whispering-gallery modes Part I: Basics", IEEE J. Sel. Topics Quantum Electron. 12, 3-14 (2006), https://doi.org/10.1109/JSTQE.2005.862943
37. A.V. Kanaev, V.N. Astratov, W. Cai, "Optical coupling at a distance between detuned spherical cavities," Appl. Phys. Lett. 88, 111111 (2006): https://doi.org/10.1063/1.2186075
38. Y.E. Geints, I.V. Minin, and O. V. Minin, "Coupled Optical Resonances in a Dielectric Microsphere: Physical Concept of a Miniature Optical Pressure Sensor," Atmospheric and Oceanic Optics 35, No. 6, 802–810 (2022): DOI: 10.1134/S1024856022060112.